Optical CMOS Transceiver with 8×32 SPAD array, 32 TDCs and Laser Diode Driver for Wearable Time-Domain Diffuse Optics Applications

Jan Nissinen, Marko Pakaslahti, Tore Leikanger, Juha Häkkinen, Jaakko Huikari and Ilkka Nissinen, *Member IEEE*
Circuits and Systems Research Unit, University of Oulu, Oulu, Finland
jan.nissinen@oulu.fi

***Abstract*—A single-chip optical transceiver for wearable time-domain diffuse optics healthcare applications has been fabricated in 150 nm CMOS technology. The chip includes an 8×32 single-photon avalanche diode (SPAD) array with 32 time-to-digital converters (TDC) with ~60 ps resolution and a laser diode driver which can produce short ~0.5 A current pulses at a repetition rate of 15 MHz. The measured instrument response function (IRF) of the transceiver was measured to be ~120 ps with a laser pulse width of 90 ps and a wavelength of 854 nm.**

Keywords—Time-correlated single-photon counting, Laser diode, Single-photon avalanche diode

I. Introduction

Visible and near-infrared light is a promising source in the range of non-ionizing radiation to characterize highly scattering turbid media like biological tissues and thus for enabling in vivo tissue diagnosis, and tissue oxygenation and blood volume variation measurements [1]. Diffuse optics (DO) utilize light to probe subcutaneous (depth ~2–4 cm) human tissues safely to solve the optical properties and structure of the tissue. Due to the thickness of human tissues, the reflectance mode is normally used where an optical source (laser) and a sensor are on the same side of the tissue, as shown in Fig. 1 a).

There are several options how DO can be utilized for collecting information from the tissue, such as continuous wave (CW), frequency domain (FD) and time domain (TD) [2]. CW and FD based solutions benefit from their simple structures and inexpensive components. However, CW techniques can only measure relative changes of tissue chromophore concentrations. Contrary to CW solutions, FD and TD techniques can separate the absorption from scattering to achieve more precise characterization of the optical properties of the tissue [2]. Moreover, the TD technique has a unique property for the selection of different average depths to be investigated by measuring the time-of-arrival of the backscattered photons and, thus reaches a deeper part of the tissue compared to the FD technique [2]. In Fig. 1 a) and b), the basic principle of the TD technique is shown where a short optical pulse (~100 ps) is transmitted to a tissue and a photodetector with a time interval measurement unit (TDC) is measuring the distribution of time-of-flight (DTOF) of the backscattered photons. For example, photons which have reached the muscle tissue will be detected later than photons from fat, as shown in Fig. 1 b).

One main disadvantage of the TD technique has been expensive and bulky components such as photo multiplier tubes (PMT), picosecond laser sources and time-correlated single-photon counting electronics which has a limited TD technique to spread in wearable applications [3]. During last decades the development of the CMOS technology with single-photon avalanche diodes (SPAD) have enabled the fabrication of large arrays of SPADs and timing-electronics into a single CMOS chip for different applications [4,5,6]. In addition, semiconductor laser diodes can be driven by drivers fabricated in CMOS technology [7,8].

In [9], the TD technique is utilized for achieving a backpack system with two laser diodes to measure tissue oxygenation saturation during exercise. However, the system is still bulky and cannot be integrated into sports watches, for example. In [10] TD fNIRS system is proposed to measure brain activity where altogether 52 modules are attached to a helmet. The form factor of a single module (27 cm^3) is still big to be integrated into sports watches because of different PCBs needed for both the receiver and the transmitter. A time-gated system based on a SPAD and a vertical-cavity surface-emitting laser VCSEL are presented in [11] where all transceiver components have been packaged in a 12 mm x 12 mm QFN package. However, only a predefined gate window can be enabled to collect backscattered photons and thus prevent the evaluation of absorption and scattering coefficients [11].

In this work, a fully integrated transceiver IC is presented with measurement results. The transceiver IC includes a laser diode driver, a time-gated 8×32 SPAD array and 32 TDCs integrated in a single 150 nm CMOS chip which can be used in wearable healthcare applications. This is the first paper where, to the best of our knowledge, a fully integrated optical transceiver is presented.

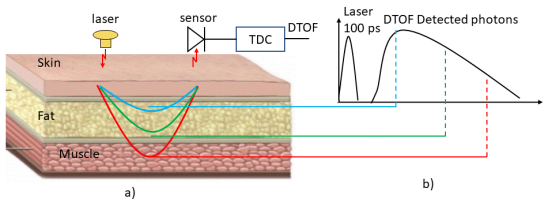

Fig. 1. a) Principle of diffuse optics in reflectance mode and b) a transmitted optical pulse and detected distribution times of flight of backscattered photons in time-domain diffuse optics.

II. Time-Domain Diffuse Optics Transceiver

A block diagram of the time-domain diffuse optics transceiver IC is shown in Fig. 2. The transceiver IC consists of a laser diode driver (LDD) with the adjustable pulse width control (PWC), 8×32 SPAD array with 32 6-bit TDCs and four histogram registers (REGs) shared by 8 TDCs. An FPGA circuit controls the operation by triggering the transmitter (Trig) and simultaneously enabling SPADs (Sync) to operate in Geiger mode, in which case SPADs are ready to detect backscattered photons from a tissue. When any of the SPADs is triggered by a photon, a start timing mark is generated for a TDC and a common stop signal (stop) is generated from a sync signal after an adjustable

This work was supported by the Academy of Finland under Contract 330121 and 323719 and Business Finland under Contract 41656/31/2020 and Riitta and Jorma J. Takanen Foundation

delay (Δt stop) for all TDCs. After N pulses, the distribution of time-of-flight of backscattered photons is stored to histogram registers which then can be read by the FPGA using a 16-bit bus (Data) and 2-bit address for registers. In addition, a serial-in parallel-out (SIPO) register has been used to control all delays (Δt stop and Δt TG), a pulse width of the laser and hot pixel eliminations.

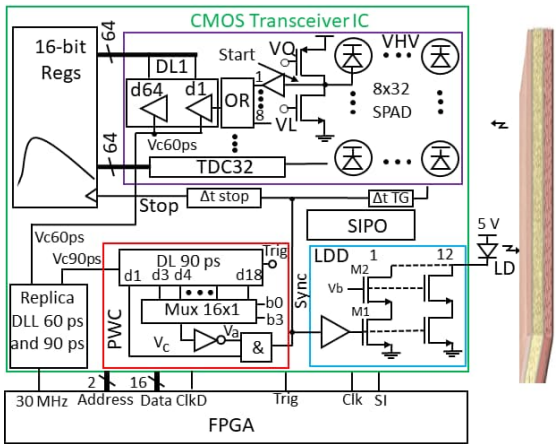

Fig. 2. A block diagram of the transceiver for time-domain diffuse optics.

A. 8×32 SPAD array with 32 TDCs

The SPAD array consists of 8 columns and 32 rows so that one TDC is connected to each row, as shown in Fig. 2. Each SPAD in a row has its own load and quench transistors (VL and VQ) which are controlled by a Sync signal with an adjustable delay (Δt TG and Sync in Fig. 2) from the laser driver. 8 SPADs have been connected via buffers to an OR gate so that any of the SPADs, triggered by a photon, generate a timing mark which starts to propagate through the delay line (DL1) with 64 elements. A common Stop signal with an adjustable delay (see Fig. 2, Δt stop) is used for storing the states of the delay lines (one hot code) to 64 16-bit ripple counter registers after each laser pulse to form a DTOF histogram of the detected photons after N amount of laser pulses. One ripple counter register has been shared by 8 DLs. To store the results of the 32 rows, four ripple counter registers are needed. After N amount of laser pulses, the results of the ripple counters are read by FPGA.

At the beginning of the operation, SPADs are quenched (VQ = 0 V) and VL is at 0 V so that anode nodes of the SPADs are at 3.3 V. Then, the VQ signal is set to 3.3 V and, after a short delay, VL is set to 3.3 V in which case anodes of the SPADs are discharged to 0 V. Now the SPADs are biased in Geiger mode when VHV (cathode node) is selected to be ~3.3 V above the breakdown voltage of the SPAD. When any of the SPADs is triggered by a photon, the rising edge starts to propagate through the delay line and finally the state of the delay is stored by the global Stop signal synchronized to the laser trig signal (Sync) with an adjustable delay (Δt stop), as shown in Fig. 2.

TDCs are based on delay lines which are stabilized using the control voltage from a replica delay locked loop [5]. A 30 MHz reference signal is used for stabilizing the delay of a single element to 60 ps (Replica DLL 60 ps in Fig. 2). The control voltage of the replica DLL (V_{c60ps}) is used for controlling any similar delay elements of all the DLs of TDCs.

B. Laser diode driver with pulse width control

A simplified schematic of the laser diode driver is shown in Fig. 2. The driver is based on cascode-connected M1 (1.8 V) and M2 (5 V) transistors which are producing current pulse through the laser diode (LD) [8]. The amplitude of the current pulse can be controlled by adjusting an off-chip voltage (vb) at the gate of M2. The transistor M1 acts as a switch and the width of a trigger signal at the gate of M1 is defining the width of the current pulse. Altogether 12 cascode-connected transistors are driving the laser diode via 12 I/O pads to decrease the total inductance of the current loop.

A delay line (DL 90 ps) and 4-bit MUX can be used for adjusting the width of the trigger signal. The first rising edge of the delay line (V_c) goes directly to the AND gate and the delayed rising edge selected by 4-bit control word (b0…b3) goes via inverter to another input of the AND gate (V_a) to form a pulse with an adjustable width. A DL of 90 ps is stabilized by the control voltage (Vc90ps in Fig. 2) from the replica delay line having a locked delay of 90 ps, resulting in a pulse width adjustment resolution of 90 ps.

III. Measurements Results

The fabricated time-resolved diffuse optics module based on the designed 150 nm CMOS (Lfoundry) transceiver IC is shown in Fig. 3. The size of the CMOS transceiver chip is 6 mm x 5 mm and it has been bonded to a test PCB. The total active area of the SPAD array is 0.1 mm^2 and has a fill factor of 28%, and it is offered by foundry. The breakdown voltage of the SPAD is about 18 V and the excess bias of 2.8 V has been used in all measurements. Moreover, a sample rate of 50 Hz has been achieved when 20,000 pulses have been transmitted to the target at the repetition rate of 15 MHz, and after that histogram registers have been read by FPGA before the next sample (causing dead time). In that case, the power consumption of the transceiver was 25 mW, also including level shifters between FPGA and IC (1.8 V<->3.3 V).

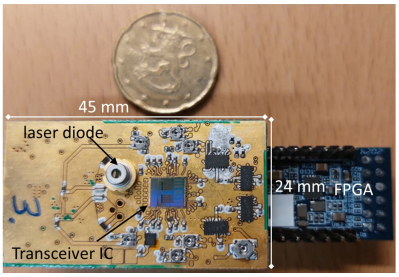

Fig. 3. The test PCB with a transceiver IC, a laser diode and FPGA board.

A. Laser driver measurements

The laser driver was designed so that the width of the current pulse could be adjusted to be suitable for different kinds of laser diodes for producing narrow optical pulses (full width half maximum, FWHM ~100 ps). Firstly, the stability of the pulse width adjustment was measured by using a 10 Ω resistor as the load of the driver. The width of the current pulse can be adjusted by the 4-bit digital word with a resolution of 90 ps. As can be seen in Fig. 4, the pulse width increases monotonically from 960 ps to 1590 ps at steps of ~90 ps when a control word has been increased by one LSB in every step. When pulse widths of 720 ps or

shorter are used, the slew rate of the driver starts to deteriorate the amplitude of the pulse, as shown in Fig. 4. The amplitudes of the current pulses are approximately 500 mA (5 V/10 Ω=0.5A) at the wider pulse widths.

In optical pulse measurements, a laser diode (854 nm) in TO-56 package was used and the width of the current pulse was selected so that only the gain switching peak of the laser diode was seen with a minimum ringing in the trailing edge of a pulse. Optical pulses measured by 25 GHz detector and 35 GHz oscilloscope are shown in Fig. 5 with three different control words to see the effect of the current pulse width to the trailing edge of the optical pulse.

The average optical power was also measured at 15 MHz repetition rate, and that value was used for approximating the peak optical power when the width of the optical pulse was selected to be 90 ps (red curve in Fig. 5). The measured average power and calculated peak optical power were approximately 1.67 mW and 1.2 W, respectively.

B. Measurement of the 8×32 SPAD array with 32 TDCs

The instrument response function (IRF) of the whole transceiver was measured by using the on-chip laser driver and 854 nm laser diode and the optical pulse width of 90 ps. In the measurement, the designed SPAD array was as a detector and the optical pulse was transmitted to a target (black paper) at two distances of ~9 cm and 17 cm to define the resolution of the TDCs. The times-of-flight (TOF) of the reflected echo signals were measured by every eighth row of the 32 SPAD rows (8×32 array) and the corresponding TDC of the row (TDC1, TDC9, TDC17 and TDC25) because four ripple counter registers were shared for 32 rows. All other SPADs were disabled in the measurements. The timing skew of the array could be minimized in this case when deriving the resolution of the TDCs. The IRFs of four rows (TDCs) are shown at two different distances (9 cm and 17 cm) in Fig. 6. The mean times-of-flight at both distances were calculated from the distributions. The distance difference of 8 cm corresponds to 8 cm*66.67 ps/cm =533 ps (round trip) and from Fig. 6 we can derive the distance difference of 47.86 LSBs-38.93 LSBs=8.93 LSBs and, thus the LSB = 533 ps/8.93≈60 ps. The FWHM values of IRFs of all 4 rows were approximately 120 ps.

The linearity of the 32 TDCs was measured by using moderate background light to keep a photon detection probability of less than 5%, and SPAD array was enabled $6*10^6$ times to achieve a sufficient number of photons. The DNL of all 32 TDCs and INL of the three worst TDCs are shown in Fig. 9. The DNLs are less than +/-0.25 LSB (+/-15 ps, after the peak in the beginning caused by enabling the signal of the SPADs).

IV. Conclusion

A fully integrated CMOS transceiver for time domain diffuse optics has been presented. The proposed IC includes an 8×32 SPAD array with 32 TDCs, achieving the resolution and range of 60 ps and 6-bit and a laser diode driver which can produce ampere scale current pulses with adjustable pulse widths. The IRF (FWHM) of the transceiver was measured to be 120 ps, which is better than, for example, the state-of-the art transceiver proposed in [10] (200 ps). This kind of a single chip optical transceiver will pave the way for fabricating a small-sized micromodule for wearable battery-operated healthcare applications. To the best knowledge of the authors this is the first single chip optical transceiver for wearable time-domain diffuse optics applications.

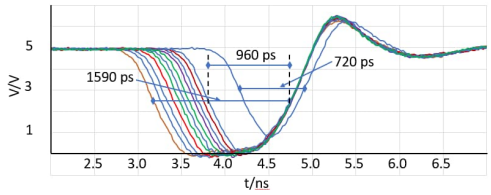

Fig. 4. Voltage pulses over a 10 Ω resistor at different pulse widths (not showing all pulse widths to keep Fig. 6 clearer).

Fig. 5. Optical pulses at three different current pulse widths.

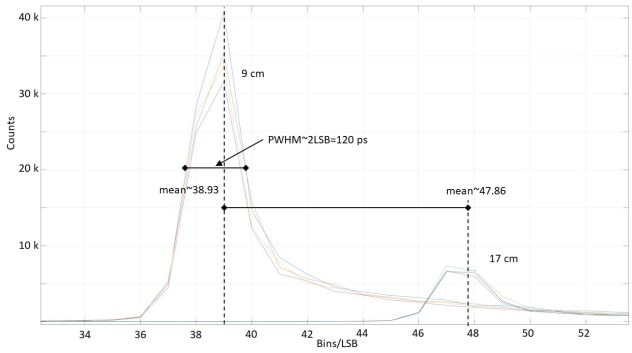

Fig. 6. A TOF measurement result at two different distances (9 cm and 17 cm).

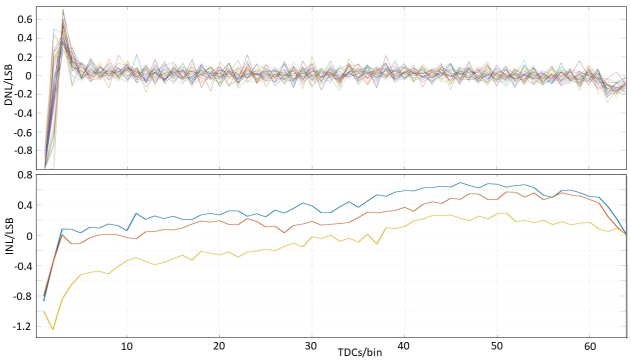

Fig. 7. The DNL of all TDCs and INL of the worst TDCs.

Acknowledgment

The authors would like to acknowledge Fondazione Bruno Kessler for designing the SPAD used in this work.

REFERENCES

[1] T. Durduran, R. Choe, W. B. Baker and A. G. Yodh, “Diffuse optics for tissue monitoring and tomography,” Rep. Prog. Phys., vol. 73, no. 7, 076701, 2010.

[2] L. Di Sieno et al., ” Time-domain diffuse optical tomography using silicon photomultipliers: feasibility study,” J. Biomed. Opt. vol. 21, no. 11, 116002, 2016.

[3] A. Pifferi et al.,” New frontiers in time-domain diffuse optics, a review,” J. Biomed. Opt. vol. 21, no. 9, 091310, 2016.

[4] A. C. Ulku et al., “A 512×512 SPAD image sensor with integrated gating for widefield FLIM,” IEEE J. Sel. Top. Quantum Electron., vol.25, no. 1, art no. 6801212, 2019.

[5] T. Talala, E. Parkkinen and I. Nissinen, “CMOS SPAD Line Sensor With Fine-Tunable Parallel Connected Time-to-Digital Converters for Raman Spectroscopy,” IEEE Journal of Solid-State Circuits, Early Access, 2022, doi: 10.1109/JSSC.2022.3212549.

[6] R. K. Henderson et al.,” A 192×128 Time Correlated Single Photon Counting Imager in 40nm CMOS Technology,” IEEE 44th European Solid State Circuits Conference (ESSCIRC), Dresden, Germany, pp. 54-57, 2018.

[7] L. Di Sieno et al., “Miniaturized pulsed laser source for time-domain diffuse optics routes to wearable devices,” J. Biomed. Opt. vol. 22, no. 8, 085004, 2017

[8] G. Blasco et al. “A Sub-ns integrated CMOS laser driver With configurable laser pulses for time-of-flight applications,” IEEE Sensors Journal, vol. 18, no. 16, pp. 6547-6556, 2018

[9] M. Lacerenza et al., ”Wearable and wireless time-domain near-infrared spectroscopy system for brain and muscle hemodynamic monitoring,” Biomed. Opt. Express., vol.11, no.10, pp. 5934-5949, 2020.

[10] H. Y. Ban et al., ”Kernel Flow: a high channel count scalable time-domain functional near-infrared spectroscopy system,” J. Biomed. Opt. vol. 27, no. 7, 074710, 2020.

[11] S. Saha, Y. Lu, S. Weyers, F. Lesage and M. Sawan, "Compact optical probe for time-resolved NIRS-Imaging," in IEEE Sensors Journal, vol. 20, no. 11, pp. 6101-6113, 2020.